Science of the Total Environment 876 (2023) 162587

Contents lists available at ScienceDirect

Science of the Total Environment

journal homepage: www.elsevier.com/locate/scitotenv

Adipogenic and endocrine disrupting mixture effects of organic and inorganic pollutant mixtures

Roxanne Bérubé [a,1], Matthew K. LeFauve [a,1], Samantha Heldman [a], Yu-Ting Tiffany Chiang [a], Johnna Birbeck [b], Judy Westrick [b], Kate Hoffman [c], Christopher D. Kassotis [a,*]

[a] Institute of Environmental Health Sciences and Department of Pharmacology, Wayne State University, Detroit, MI 48202, United States of America
[b] Department of Chemistry, Wayne State University, Detroit, MI 48202, United States of America
[c] Nicholas School of the Environment, Duke University, Durham, NC 27708, United States of America

HIGHLIGHTS

- Assessed potential combination effects of inorganic and organic contaminant mixtures.
- Greater than expected activity observed for mixtures on nuclear receptor bioactivities.
- Greater than expected activity observed for mixtures on adipogenesis in human mesenchymal stem cells.
- Results support further testing of more complex contaminant mixtures that better reflect environmental exposures.

GRAPHICAL ABSTRACT

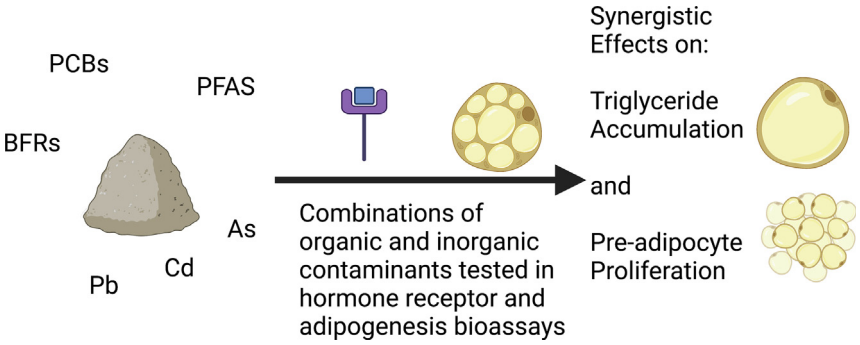

ARTICLE INFO

Editor: Jay Gan

Keywords:
Endocrine disrupting chemicals
Adipogenesis
Obesogen
Obesity
Metabolic disruption
House dust

ABSTRACT

Chronic health conditions are rapidly increasing in prevalence and cost to society worldwide: in the US, >42 % of adults aged 20 and older are currently classified as obese. Exposure to endocrine disrupting chemicals (EDCs) has been implicated as a causal factor; some EDCs, termed "obesogens", can increase weight and lipid accumulation and/or perturb metabolic homeostasis. This project aimed to assess the potential combination effects of diverse inorganic and organic contaminant mixtures, which more closely reflect environmentally realistic exposures, on nuclear receptor activation/inhibition and adipocyte differentiation. Herein, we focused on two polychlorinated biphenyls (PCB-77 and 153), two perfluoroalkyl substances (PFOA and PFOS), two brominated flame retardants (PBB-153 and BDE-47), and three inorganic contaminants (lead, arsenic, and cadmium). We examined adipogenesis using human mesenchymal stem cells and receptor bioactivities using luciferase reporter gene assays in human cell lines. We observed significantly greater effects for several receptor bioactivities by various contaminant mixtures relative to individual components. All nine contaminants promoted triglyceride accumulation and/or pre-adipocyte proliferation in human mesenchymal stem cells. Comparing simple component mixtures to individual components at 10 % and 50 % effect levels revealed putative synergistic effects for each of the mixtures for at least one of the concentrations relative to the individual component chemicals, some of which also exhibited significantly greater effects than the component contaminants. Our results support further testing of more realistic and complex contaminant mixtures that better reflect environmental exposures, in order to more conclusively define mixture responses both in vitro and in vivo.

* Corresponding author at: Institute of Environmental Health Sciences and Department of Pharmacology, School of Medicine, Wayne State University, 2111 Integrative Biosciences Center, 6135 Woodward Avenue, Detroit, MI 48236, United States of America.
E-mail address: christopher.kassotis@wayne.edu (C.D. Kassotis).
[1] Co-first authors; both authors contributed equally to this manuscript.

http://dx.doi.org/10.1016/j.scitotenv.2023.162587
Received 10 October 2022; Received in revised form 22 February 2023; Accepted 27 February 2023
Available online 05 March 2023

1. Introduction

Humans are regularly exposed to complex mixtures of endocrine disrupting chemicals (EDCs), beginning as early as gestation (Dallaire et al., 2003; Houlihan et al., 2005) and continuing throughout our lives (Environmental Protection Agency (EPA), 2017; Fraser et al., 2012; Landrigan et al., 2002; Mogensen et al., 2015; Rudel et al., 2003; Watkins et al., 2013). EDCs are able to disrupt normal hormonal action (Diamanti-Kandarakis et al., 2009; Gore et al., 2015), and have been demonstrated to contribute to adverse health risks in humans and animals (Rudel et al., 2003; Stapleton et al., 2006; Stapleton et al., 2009). Metabolism disrupting chemicals (MDCs) have been demonstrated to disrupt metabolic health via disruption of weight gain, adiposity, glucose/insulin signaling, and/or other mechanisms (Heindel et al., 2017; Heindel et al., 2022; Heindel et al., 2015; Kassotis et al., 2022b; Lustig et al., 2022), some of which have been shown to occur through endocrine mechanisms (Fang et al., 2015a; Fang et al., 2015b; Fang et al., 2015c; Kassotis et al., 2020; Kassotis et al., 2018a; Kassotis et al., 2019; Kassotis et al., 2018b). Our understanding of health outcomes linked with chemical exposures is limited, and has primarily focused on single chemicals and often with high concentrations that do not accurately reflect realistic environmental exposures (Martin et al., 2021). Limited research has evaluated more complex chemicals mixtures (Martin et al., 2021), particularly mixtures comprised of both inorganic and organic contaminant components. Given we know that humans are routinely exposed to between hundreds and thousands of chemicals daily (Hoffman et al., 2018; Kassotis et al., 2016; Lyche et al., 2010; Phillips et al., 2018; Schilmann et al., 2010), characterizing the effects of realistic, complex environmental mixtures is of profound importance.

One environmental mixture that represents a chronic exposure source is household dust, which is a reservoir for thousands of chemicals that leach from consumer products and building materials in the home (e.g., phthalates, flame retardants, pesticides, polycyclic aromatic hydrocarbons, phenols, and perfluoroalkyl substances (PFAS)) (Kademoglou et al., 2017; Mitro et al., 2016; Rasmussen et al., 2013; Rudel et al., 2003; Stapleton et al., 2008; Stapleton et al., 2005; Stapleton et al., 2006; Stapleton et al., 2009; Suzuki et al., 2007; Suzuki et al., 2013). Many of the chemicals commonly reported in household dust are MDCs (Heindel et al., 2017; Heindel et al., 2022; Heindel et al., 2015; Kassotis et al., 2022b; Lustig et al., 2022), and/or EDCs (Chou et al., 2015; Fang et al., 2015a; Fang et al., 2015b; Fang et al., 2015c; Kollitz et al., 2018; Suzuki et al., 2007). We have previously shown that low concentrations of many household dust samples promote robust adipocyte differentiation and proliferate precursor cells in vitro (Kassotis et al., 2019). The extent of dust-induced triglyceride accumulation was significantly and positively correlated with a number of individual semi-volatile organic contaminants (SVOCs) (Kassotis et al., 2021a; Kassotis et al., 2019). We also assessed whether mixtures of SVOCs might be responsible for the adipogenic effects; while we reported greater effects for the SVOC mixture than for individual components (Kassotis et al., 2021a), we could not explain the bulk of the observed adipogenic activity. This suggested that there might be underexplored contaminants in these mixtures that might be contributing to the observed bioactivities. We also reported significant, positive associations between house dust-induced triglyceride accumulation in vitro and the body mass index (BMI) of adult residents (Kassotis et al., 2019). Given that the US EPA estimates that children ingest 60–100 mg of indoor dust per day (Environmental Protection Agency (EPA), 2017), contributing to increased child body burdens for diverse contaminants (Dixon et al., 2009; Stapleton et al., 2012; Watkins et al., 2011; Watkins et al., 2012), determination of mixture effects for these common co-occurring contaminants is urgently needed.

To start addressing this question, we composed mixtures of common co-occurring organic and inorganic contaminants, with particular relevance to Michigan, United States. SVOCs were selected based on high frequency of detection in residential household dust samples (Kassotis et al., 2021a), and included two polychlorinated biphenyls (PCBs; PCB-77 and 153), two PFAS (perfluorooctanoic acid (PFOA) and perfluorooctanesulfonic acid (PFOS)), two brominated flame retardants (BFRs; 2,2′,4,4′-tetrabromodiphenyl ether (BDE-47) and 2,2′,4,4′,5,5′-hexabromobiphenyl (PBB-153)), and three inorganic contaminants (lead, arsenic, and cadmium). These contaminants have been reported to co-occur in household dust with high frequencies (Table S1) and there are previous reports of many of these chemicals as MDCs (Green et al., 2018; Martini et al., 2018; Rodriguez et al., 2020; Taxvig et al., 2012; Tung et al., 2014; Watkins et al., 2015), suggesting potential for mixture effects on metabolic outcomes. Specifically, average concentrations of arsenic ranged from 1600 to 62,000 ng/g, average lead concentrations ranged from 49,100–573,000 ng/g, and average concentrations of cadmium were 1100–1,900,000 ng/g (Table S1). Concentrations of organic pollutants were approximately 100 times lower than the inorganic contaminants in most studies, with the highest reported concentrations for BDE-47 and PFOA, and very limited data available for PBB-153 and PCB-77 (Table S1). Michigan has particularly high exposures of PBB-153 following an agricultural accident in 1973–1974, when “FireMaster”, a mixture of PBBs, was accidentally added to cattle feed in place of “NutriMaster”, a nutritional supplement, contaminating diverse agricultural products and highly exposing the population of Michigan (Di Carlo et al., 1978; Jones et al., 1975; Robertson and Chynoweth, 1975). Four decades later, exposed residents still maintain higher levels of specific PBBs (e.g., PBB-153) than the rest of the US, and Michiganders born after the incident, while lower than the exposed Michiganders, still have higher PBB levels than the general US population (Chang et al., 2020).

As such, the goals of this study were to assess potential mixture effects underlying interactions between diverse and complex co-occurring contaminant mixtures on adipogenic outcomes through a broad scope. We examined each of these nine contaminants individually, along with 10 mixtures of various combinations of them: PFAS mixture, BFR mixture, PCB mixture, inorganic mixture, PFAS + inorganic mixture, BFR + inorganic mixture, PCB + inorganic mixture, organic mixture (all six organics), a total mixture (all nine contaminants), and an environmental mixture (all nine contaminants) that approximated relative proportions of these contaminants as reported in household dust samples (e.g., with a 100-fold difference between organic and inorganic concentrations). Each chemical and mixture of chemicals were examined for adipogenic activity using human mesenchymal stem cells and murine 3T3-L1 cells as well as for receptor bioactivities (agonism and antagonism) on several known adipogenic pathways (Kassotis et al., 2017b; Li et al., 2011; Shao et al., 2016), including peroxisome proliferator activated receptor gamma (PPARγ), retinoid X receptor alpha (RXRα), glucocorticoid receptor (GR), and thyroid receptor beta (TRβ). We examined mixture effects as predicted by the concentration addition model and compared these predictive model results with measured responses from bioassays. We also measured concentrations of inorganic contaminants in a subset of household dust samples and correlated these concentrations with previously measured adipogenic and receptor bioactivities.

2. Materials and methods

2.1. Chemicals

Chemicals for use in bioassays were purchased as follows: rosiglitazone (peroxisome proliferator activated receptor gamma, PPARγ, agonist; Sigma cat # R2408, ≥98 %), T0070907 (PPARγ antagonist; cat # R2408, ≥98 %), triiodothyronine (T3; thyroid hormone receptor beta, TRβ, agonist; VWR cat # 80057–656, ≥98 %), 1–850 (TRβ antagonist; Millipore cat # 609315, ≥98 %), dexamethasone (glucocorticoid receptor, GR, agonist; D4902-25MG), mifepristone (GR antagonist; M8046-100MG), LG100268 (retinoid X receptor alpha, RXRα, agonist; SML0279-5MG), and HX531 (RXRα antagonist; SML2170-5MG). Stock solutions were prepared in 100 % DMSO (Sigma cat # D2650) and stored at −20 °C between uses. Details of test chemicals are provided in Table S2. Mixtures of chemicals were comprised of equimolar concentrations of contaminants,

including the PFAS mix (combination of the two PFAS), the BFR mix (combination of the two BFRs), the PCB mix (combination of the two PCBs), a PFAS + inorganic mix (both PFAS and three inorganics), a BFR + inorganic mix (both BFRs and the three inorganics), a PCB + inorganic mix (both PCBs and the three inorganics), an inorganic mix (all three inorganics), an organic mix (all six organics), and a total mix (all six organics and three inorganics). Throughout the manuscript, a 1 μM mixture concentration will be used to denote 1 μM of each of the component chemicals rather than the summed concentration of the components. An additional environmental mix was designed of all 9 contaminants, with the inorganics at 100-fold higher concentrations than the organics to reflect the average proportional difference between these inorganics and organics as described in the literature (Table S1). A description of each mixture is detailed in Table S3.

2.2. Reporter gene activity bioassays

HEK-293T/17 human embryonic kidney cells were purchased from the ATCC (cat# CRL-11268, lot# 70022180) and were maintained in growth media (DMEM-HG, Gibco #11995, with 10 % fetal bovine serum, Sigma F2442-500ML, and 1 % penicillin and streptomycin, Gibco 15140), ensuring cells did not reach confluency. Ishikawa endometrial adenocarcinoma cells were purchased from Sigma (cat# 99040201, lot# 17C011) and were maintained in growth media (MEM, Gibco 11090, with 5 % newborn calf serum, Fisher 16010159, 1 % glutamax, Gibco 35050, 1 % non-essential amino acids, Gibco 11140, and 1 % penicillin and streptomycin). Near confluent flasks were switched to white medium (same base media without phenol red, and with charcoal-stripped fetal bovine serum) at least two days prior to transfection. To transfect, flasks were treated with a combination of Lipofectamine LTX & Plus reagent (Invitrogen cat# 15338-100) and plasmids in Opti-MEM (Gibco 11058), then recovered overnight in white assay media (media without phenol red). Plasmids consisted of human hormone receptor constructs (PPARγ: pcDNA-PPARγ1, TRβ: hTRβ1-pSG5, GR: pRST7-GR, RXRα: pcDNA-RXRα), reporter gene plasmids (PPARγ: DR1-luciferase, TRβ: pGL4-TK-2X-TADR4, GR: MMTV-luciferase, RXRα: DR1-luciferase), and a constitutively-active CMV-β-Gal normalization plasmid (all plasmids were generous gifts of the Donald McDonnell Lab). PPARγ, RXRα, and TRβ plasmids were transfected into HEK293 cells and GR into Ishikawa cells. The following morning, transfected cells were seeded at approximately 60,000 cells per well into 96-well tissue culture plates and allowed to settle for several hours. Plated cells were then induced with dose responses of positive and/or negative controls and test chemicals using a 0.1 % DMSO vehicle. Cells were treated for approximately 18–24 h and then lysed for luciferase and beta galactosidase assays.

Raw luminescence values were converted to fold inductions relative to the solvent control responses (0.1 % DMSO) and then were used to calculate percent bioactivities relative to positive control agonists and/or antagonists. For agonist bioassays, chemical values were compared to the maximal positive control responses to determine percent activity. For antagonist bioassays, percent activity was calculated as percent enhancement or suppression relative to the half maximal positive control responses. Significant reduction in constitutively active beta galactosidase promoter activity ($\geq$15 %) was used as an indirect marker of toxicity and receptor bioactivities were only reported in the absence of this presumed toxicity.

2.3. Adipogenesis cell care and bioassays

Human bone marrow mesenchymal stem cells (hMSCs) were purchased from Lonza (catalog # PT-2501; lot # 155677; passage 2). Cells were maintained as suggested by manufacturer in manufacturer-specific mesenchymal stem cell basal growth media (Lonza catalog # PT-3001). 3T3-L1 cells (Zenbio cat# SP-L1-F, lot# 3T3062104) were maintained in pre-adipocyte media (Dulbecco's Modified Eagle Medium – High Glucose; DMEM-HG; Gibco cat# 11995, supplemented with 10 % bovine calf serum and 1 % penicillin and streptomycin) (Kassotis et al., 2017b). Cells were maintained in a sub-confluent state until differentiation and each thaw of frozen cells was utilized within three passages, with no appreciable modulation in response observed (i.e., positive and negative control responses compared across each biological replicate).

hMSCs and pre-adipocytes were induced to differentiate as described in detail previously (Kassotis et al., 2022a). Briefly, cells were seeded in provider-specific basal media into 96-well tissue culture plates (Greiner catalog # 655090) at 10–30,000 cells per well. Once confluent (for 3T3-L1 cells, a further 48-hour window was allowed between confluency and differentiation induction), differentiation was induced by replacing basal media with test chemicals and/or controls using a 0.1 % DMSO vehicle in differentiation media (Lonza catalog # PT-3102B; 3T3: DMEM-HG with 10 % fetal bovine serum, 1 % penicillin/streptomycin, 1.0 μg/mL human insulin, and 0.5 mM 3-isobutyl-1-methylxanthine, IBMX). Lonza cells were differentiated with three rounds of differentiation induction, according to company instructions and as reported previously (Kassotis et al., 2022a). Specifically, cells were treated with differentiation media and test chemicals for three days, then switched to adipocyte maintenance media (Lonza catalog # PT-3102A) for three days. This cycle was repeated twice more (three days differentiation media and three days adipocyte maintenance media, each with fresh test chemical dilutions) and then maintained in adipocyte maintenance media, with media and test chemical changes every 3–4 days, until 21 days after the initial induction, when plates were assayed. 3T3-L1 cells were differentiated for 48 h and then media was replaced with fresh exposures diluted in adipocyte maintenance media (differentiation media without IBMX). This media was refreshed every 2–3 days, until 10 days after the initial induction, when plates were assayed.

To assay plates, media was removed from all wells and cells were rinsed with Dulbecco's phosphate-buffered saline (DPBS) and then removed. Dye mixture was then added to each well (200 μL; 19 mL DPBS, 20 drops NucBlue® Live ReadyProbes® Reagent, Thermo cat # R37605, and 500 μL Nile Red solution, 40 μg/mL, Sigma cat #72485-100MG). Plates were incubated, protected from light, for 30–40 min at room temperature, then fluorescence was measured using a Molecular Devices SpectraMax iD5 microplate spectrofluorimeter (485 nm/572 nm excitation/emission for Nile Red and 360/460 for NucBlue). Triglyceride accumulation was calculated first as fold induction of individual chemical responses over the intra-assay differentiated vehicle control responses (0.1 % DMSO) and then as percent activities relative to the maximal rosiglitazone-induced response. DNA content was calculated as percent deviation from the differentiated vehicle control responses (positive values, pre-adipocyte proliferation; negative values, cytotoxicity), and then was used to normalize total triglyceride accumulation per well to triglyceride accumulation per DNA content. Three biological replicates (separate assays and cell line passages), each including four technical replicates (replicates within a single plate of a single assay), were performed for each cell line and test chemical. Chemical placement was randomized across plates and assays, and included both positive and negative controls in every plate across several locations to foster reproducibility. Efficacies and potencies were determined as above. Assay performance: 3T3-L1, intra-assay Z′-factor: 0.70–0.85; signal/noise: ~5.4-fold change, mean CV range: 11.1–17.3 %; hMSCs, intra-assay Z′-factor: 0.62–0.74; signal/noise: ~3.9-fold change, mean CV range: 7.9–14.2 %.

2.4. Dust sample collection and processing

Anonymized dust samples were collected from central NC and processed as described previously (Kassotis et al., 2019; Kollitz et al., 2018). These dust samples were previously tested for adipogenic activity using 3T3-L1 cells and for TRβ antagonism using reporter gene assays described herein. These results have been described in detail previously (Hoffman et al., 2017; Kassotis et al., 2019). A subset of these dust samples (n = 30) was processed for measurement of inorganic contaminants (lead, cadmium, and arsenic) herein, and associations made with existing bioactivity data.

2.5. Inorganic contaminant analysis in household dust samples

All solutions were made up in trace metal grade solvents. Samples (~100 mg) were digested using the following microwave digestion

procedure. The samples were added to a 10 mL digestion vessel with a Teflon liner. 1 mL of concentrated nitric acid was added to the vessel containing the sample and was allowed to sit for 1 h. A second mL of concentrated nitric acid was added, contents were swirled, and allowed digestion for another hour. Lastly, 200 μL of hydrogen peroxide was added to the vessel, swirled, and let sit overnight. The next day the vessels were capped tightly and digested using a CEM Mars 6 microwave digestor (Matthews, NC, USA). The microwave digestion method was a modified method for US EPA 3052, in which the ramping of the temperature to 180 °C was lengthened to 20 mins, and then held at 180 °C for 9.5 mins. Samples were left to cool before dilution with DI water. All ICP-MS measurements were performed on an Agilent 7700x ICP-MS (Santa Clara, CA, USA) in general purpose mode. The instrument was tuned using Agilent tuning solution for ICP-MS 7500cs using the online ICP-MS Mass Hunter Software in helium (He), high energy helium (HEHe), and hydrogen (H2) gas modes. Calibration standards were made up using standards from High Purity Standards (Charleston, SC, USA), and were diluted in a 2 % HNO3 solution (As, Cd, and Pb were analyzed for this experiment). During sample analysis, quality control samples included a blank (negative control) and a check standard (25 ppb, prepared separately from the calibration standards, positive control) and were analyzed every 10 samples.

2.6. Mixture analysis of bioassay outcomes

Predictive utility of concentration addition for the observed adipogenic effects was examined through use of the concentration addition mixture model as described previously (Rajapakse et al., 2002; Rajapakse et al., 2004; Silva et al., 2002), by summing each of the constituent chemical proportions in the mixture with effect *X*, divided by their concentrations in isolation that exhibited the same effect as the mixture, according to the concentration addition equation: $(\Sigma_{i=1}^{n} \frac{p_i}{EC_{xi}})^{-1}$ (Ermler et al., 2011).

To determine magnitude of deviations from additivity, the toxic effect summation was determined as the proportion of the observed effects to the predicted effects: Ratio $= \frac{observed\ EC_x\ (mixture)}{expected\ EC_x\ (mixture)}$ (Martin et al., 2021). This was then used to define the index of prediction quality, as described in detail previously (Martin et al., 2021), creating a linearized symmetric scale to express over- or underestimation as percentages of the ratios as below:

$$IPQ = \begin{cases} 100*(Ratio - 1)\ if\ Ratio \geq 1 \\ 100*\left(1 - \frac{1}{Ratio}\right)\ if\ Ratio < 1. \end{cases}$$

As described previously (Martin et al., 2021), an IPQ of +75 % describes an observed effect concentration that is 75 % above that of the predicted value, whereas −75 % would be an observed effect that is 75 % below the predicted value. IPQs were then used to determine effect type. IPQs between −100 % and + 100 % were deemed additive, those < −100 % were deemed antagonistic, and those > + 100 % were deemed synergistic.

2.7. Statistical analysis

Data for adipogenic and nuclear receptor bioactivities are presented as means ± standard error of the mean (SEM) from the median of four technical replicates (intra-assay replicates) from three independent biological replicates (separate assays). Lowest observed significant effect level (LOEL) and significant differences between individual contaminants and their mixtures were determined with Kruskall Wallis tests in GraphPad Prism 9 using percent activities as calculated above. Relationships between measures of adipogenic activity and activation or inhibition of specific nuclear receptors were evaluated using Spearman's correlations in GraphPad. Spearman's correlations were also performed to examine relationships between inorganic contaminant measurements in dust and bioactivities reported in these extracts previously (Kassotis et al., 2019). The principal component analysis (PCA) was computed with RStudio version 2022.02.2 and R version 4.1.1 (r-project.org, version 4.1.3). The "PCA" command from the FactoMineR package (Kassambara and Mundt, 2020) was used to perform the PCA. To present the data, the biplot, scree plot, and correlation matrix were performed with the commands "fviz_pca_biplot", "f_viz_eig" and "corrplot" from the factoextra (Kassambara and Mundt, 2020), ggplot2 (Fox and Weisberg, 2019), tidyverse (Wickham, 2016), and corrplot (Wei and Simko, 2021) packages. The dataset included the average response of each cellular assay (hMSCs and receptor bioactivities) for each individual chemical and mixtures.

3. Results

A set of common co-occurring contaminants (three inorganic and six organic) were evaluated for toxicity across endocrine receptor endpoints and for adipogenic bioactivities, both individually and in various combinations. Mixtures were evaluated for antagonistic, additive, or synergistic effects at a range of concentrations to evaluate the potential interplay of these contaminants on adipogenesis-related endpoints. Selected inorganic contaminants were measured in a randomly selected subset of anonymized household dust extracts to determine potential associations between inorganic contaminants and dust extract-induced bioactivities.

3.1. Nuclear receptor activities of individual contaminants and mixtures

Both individual contaminants and their mixtures promoted agonism and/or antagonism of the targeted hormone receptors, with the mixtures often promoting greater effects than the component contaminants (Fig. 1, Figs. S1–S5). Only the inorganic mix promoted significant GR agonism (significantly greater response than each of the individual inorganic contaminants at 1 μM, $p < 0.05$; Fig. S4), with no other individual components or mixtures significantly activating this receptor (Fig. 1A). In contrast, most contaminants antagonized GR. The inorganic mix significantly antagonized GR at 0.1 nM, and the environmental mix and BFR mix at 1 nM (Fig. 1E). At 10 nM, the PFAS mix, PFAS + inorganic mix, organic mix, PCB-77, the PCB mix, and the PCB + inorganic mix all significantly antagonized GR; at 100 nM, PCB-153, PBB-153, BDE-47, and both lead and cadmium antagonized GR; and at 1 μM, PFOA, PFOS, arsenic, and the organic mix antagonized GR. The PFAS mix promoted significantly greater GR antagonism at 100 nM relative to the individual PFAS (Fig. S1), the BFR mix had significantly greater response than component BFRs at 1 and 10 nM (Fig. S3), and the inorganic mix had greater effects on GR antagonism at 0.1 and 1 nM than components (all $p < 0.05$; Fig. S4). More effects were observed for PPARγ, with the inorganic mix activating PPARγ at 100 nM; the environmental mix and BFR mix at 1 μM; and PFOA, arsenic, PBB-153, and PCB-77 activating at 10 μM (Fig. 1B). The BFR mix had significantly greater effects on PPARγ agonism at 1 μM and the inorganic mix had greater effects at 100 nM and 1 μM ($p < 0.05$, Figs. S3–S4). Antagonism was again more significantly affected; the PFAS + inorganic mix, PCB-77, and environmental mix antagonizing PPARγ at 10 nM; the total mix, PCB + inorganic mix, and organic mix antagonizing at 100 nM; the PFAS mix, lead, cadmium, inorganic mix, and PCB mix at 1 μM, and PFOS only at 10 μM (Fig. 1F). The PFAS + inorganics mix had significantly greater effects on PPARγ antagonism at 1 μM (Fig. S1), the PCB + inorganic mix had significantly greater effects at 100 nM and 1 μM (Fig. S2), and the environmental mix had greater activity than the component organic and inorganic mixtures at 10, 100, and 1000 nM (Fig. S5). Less potent agonism was observed for RXRα; the environmental mix, PBB-153, BFR mix, BFR + inorganic mix, PCB-77, and inorganic mix significantly activated RXRα at 1 μM and arsenic only at 10 μM (Fig. 1C). The BFR + inorganics mix had greater effects on RXR agonism at 100 nM (Fig. S3). Significant RXR antagonism was observed for the organic mix at 10 nM; the BFR + inorganic mix at 100 nM; the PCB + inorganic mix, environmental mix, and lead at 1 μM; and for arsenic and cadmium at 10 μM (Fig. 1G). The PCB + inorganic mix had significantly greater effects on RXR antagonism at 1 μM (Fig. S2) and the environmental mix had greater activity at 1 μM ($p < 0.05$, Fig. S5). Lastly, for TRβ agonism, the environmental mix and BFR mix significantly activated TRβ at 100 nM; PBB-153, the inorganic mix, and PCB-77 activated TR at 1 μM; and arsenic only at 10 μM (Fig. 1D). The environmental mix

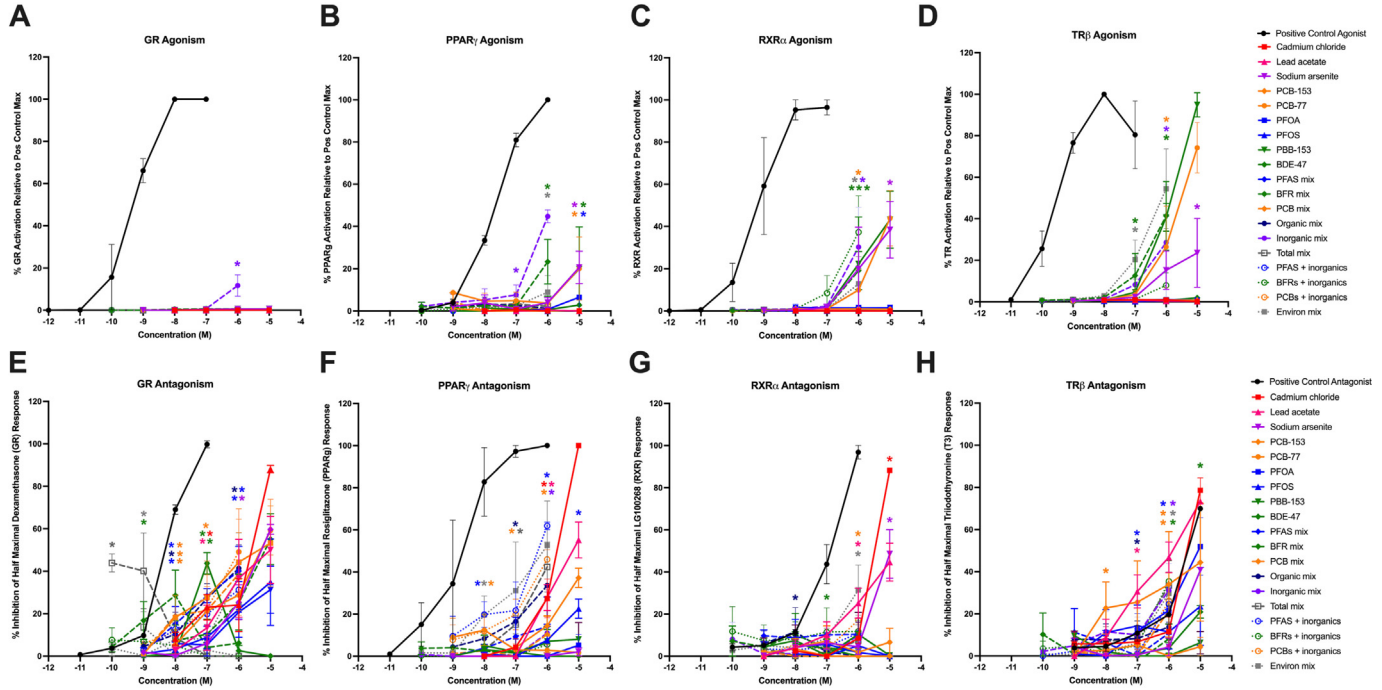

Fig. 1. Nuclear receptor bioactivities of organic and inorganic pollutants and their mixtures. Nuclear receptor bioactivities were determined following induction with standard receptor agonists and antagonists. Bioactivities reported as percent activity relative to the positive control maximum for agonist activities (A-D) and as percent enhancement or suppression of half maximal positive control response for antagonist activities (*E*-H). Receptor bioassays targeted the glucocorticoid receptor (GR; A, E), peroxisome proliferator activated receptor gamma (PPARγ; B, F), retinoid X receptor alpha (RXRα; C, G), and thyroid receptor beta (TRβ; D, H). Asterisks (*, $p < 0.05$) denote the lowest concentration for each contaminant and/or mixture with significant differences from assay baseline responses based on three biological replicates, each containing four technical replicates. PCBs = polychlorinated biphenyls, PFAS = per/poly-fluoroalkyl substances, BFRs = brominated flame retardants.

had greater activity for TR agonism at 1 μM relative to component mixtures ($p < 0.05$; Fig. S5). Antagonism of TRβ was again more pronounced; PCB-153 antagonized TR at 10 nM; PFOS, lead, and the organic mix at 100 nM; PFOA, PCB mix, PCB + inorganic mix, BFR + inorganic mix, environmental mix, and the inorganic mix at 1 μM; and BDE-47 at 10 μM (Fig. 1H). The BFR + inorganics mix had greater effects on TR antagonism at 1 μM (Fig. S3).

3.2. Adipogenic activities of individual contaminants and mixtures

Both individual PCBs (Fig. 2A, B), both PFAS (Fig. 2C, D), and each of the inorganic pollutants induced significant triglyceride accumulation in the human mesenchymal stem cell model (positive control response metrics in Fig. S6), whereas the BFRs did not (Fig. 2E, F). Of these, PCB-153 was the most active, demonstrating significant activity even at 10 nM, whereas most other contaminants induced significant effects only at 100 nM (PFOS only at 1 μM). Every mixture also promoted significant effects, and most often at lower concentrations than the individual contaminants. Specifically, the inorganic mixture promoted significant triglyceride accumulation at 1 nM; and the PFAS mix, BFR mix, PCB mix, PCB + inorganic mix, BFR + inorganic mix, organic mix, total mix, and environmental mix induced significant effects at 10 nM. The PFAS + inorganic mix induced significant effects at 100 nM only. Significantly greater effects were observed for the mixtures relative to component chemicals in several cases; the PCB mix exhibited significantly greater effects than either individual PCB at 10 nM ($p < 0.05$; Fig. 2A); the PFAS mix exhibited significantly greater effects than either individual PFAS at 10 and 100 nM ($p < 0.05$; Fig. 2C); the BFR mix exhibited significantly greater effects than either individual BFR at 10 and 100 nM ($p < 0.05$; Fig. 2E); the inorganic mix exhibited significantly greater effects than either individual inorganics at 1 nM ($p < 0.05$; Fig. 2G); the environmental mix exhibited significantly greater effects than either component organic and inorganic mixtures at 10 and 100 nM ($p < 0.05$; Fig. 2I); and the total mix exhibited significantly greater effects than either organic and inorganic mixtures at 100 nM ($p < 0.05$).

Most individual contaminants also promoted pre-adipocyte proliferation, with both PFAS, both BFRs, PCB-153, and all three inorganics promoting significant increases in DNA content relative to the differentiated solvent controls (Fig. 2). Most mixtures also promoted significant effects on pre-adipocyte proliferation, again at lower concentrations than was observed for individual contaminants. The total mix, PFAS mix, and PCB mix promoted significant increases in DNA content at 1 nM, the environmental mix, inorganic mix, and BFR mix at 10 nM, and the organic mix at 1 μM. Significantly greater effects were observed for the mixtures relative to component chemicals in several cases; the PCB mix exhibited significantly greater effects than either individual PCB at 1 and 10 nM ($p < 0.05$; Fig. 2B); the PFAS mix exhibited significantly greater effects than either individual PFAS at 1 nM ($p < 0.05$; Fig. 2D); the total mix greater than the component organic and inorganic mixtures at 1, 10, 100, and 1000 nM and the environmental mix greater than the organic and inorganic mixtures at 100 nM ($p < 0.05$; Fig. 2J).

Very different effects were observed for the same set of contaminants and mixtures in the 3T3-L1 murine pre-adipocyte model (Fig. S7). Interestingly, none of the contaminants were able to promote significant triglyceride accumulation nor pre-adipocyte proliferation (Fig. S7A, B) in 3T3-L1 cells. In contrast, most contaminants and mixtures successfully inhibited differentiation induced by a half maximal concentration of rosiglitazone as measured by reduced triglyceride accumulation (Fig. S7C) and reduced pre-adipocyte proliferation (Fig. S7D).

3.3. Associations between receptor bioactivities and adipogenic activities

Spearman's correlations were calculated to assess relationships between nuclear receptor and adipogenic bioactivities across individual contaminants and mixtures. Receptor bioactivities tended to be positively correlated with each other (Fig. 3); RXR antagonism was significantly and positively correlated with TRβ, PPARγ, and GR antagonism. These correlations were weakest with GR antagonism, which was positively correlated with RXR antagonism but not significantly correlated with TRβ or PPARγ

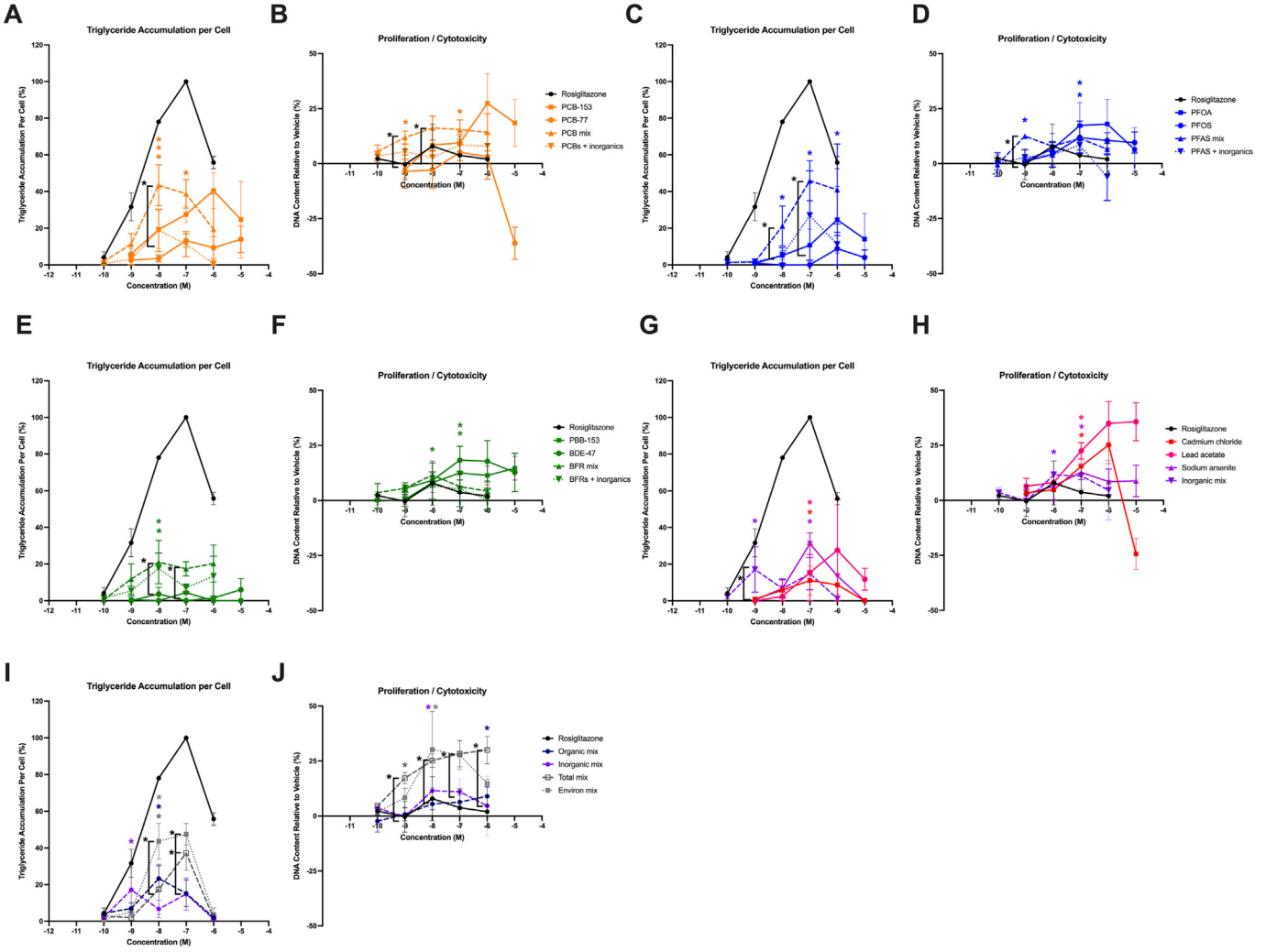

Fig. 2. Adipogenic activity of organic and inorganic pollutants and their mixtures. Human mesenchymal stem cells were induced to differentiate as described in Methods. Cells were assessed for degree of adipocyte differentiation after twenty-one days of differentiation while exposed to individual contaminants and their mixtures. Triglyceride accumulation is provided as percent of maximal rosiglitazone-induced triglyceride accumulation and normalized to DNA content (A, C, E, G, I). Proliferation/cytotoxicity is provided as percent increase or decrease in DNA content relative to differentiated solvent controls (B, D, F, H, J). Chemicals and mixtures are broken out by class to aid in clarity of presentation; individual PCBs, PCB mix, and PCB + inorganic mix are found in panels A-B, PFAS (C—D), BFRs (E-F), inorganics (G-H), and summed mixtures (I-J). PCBs = polychlorinated biphenyls, PFAS = per/poly-fluoroalkyl substances, BFRs = brominated flame retardants.
Asterisks (*, $p < 0.05$) provided in color denote the lowest concentration for each contaminant and/or mixture with significant differences from assay baseline responses, based on three biological replicates, each containing four technical replicates. Asterisks in black are paired with bars and represent significant differences between the mixture and the component chemicals. Specifically, PCB mix is significantly greater than both individual PCBs in A at 10 nM; PCB mix is greater than components at 1 and 10 nM (B); PFAS mix is greater than both components at 10 and 100 nM (C); PFAS mix greater than components at 1 nM (D); BFR mix greater than components at 10 and 100 nM (E); inorganic mix greater than components at 1 nM (G); environmental mix greater than components (organic and inorganic mixes) at 10 and 100 nM and total mix also greater at 100 nM (I); total mix greater than components (organic and inorganic) at 1, 10, 100, and 1000 nM and environmental mix at 100 nM (J).

antagonism. RXR agonism was significantly and positively correlated with TRβ, PPARγ, and GR agonism, and these associations were consistent across agonist activities for each receptor. Adipogenic activities were also interrelated; total triglyceride accumulation for each activity type (hMSC, 3T3-L1, and 3T3-L1 antagonism) was positively correlated with normalized triglyceride accumulation. Neither triglyceride accumulation nor proliferation in the hMSCs were positively associated with these metrics in 3T3-L1 cells, reflecting the disparate nature of the adipogenic results in these models for this set of chemicals and mixtures. Interestingly, normalized triglyceride accumulation in hMSCs was positively correlated with inhibited triglyceride accumulation in the 3T3-L1 antagonism model. Several interesting associations were also determined between receptor bioactivities and adipogenic activities. RXR agonism was negatively associated with total triglyceride accumulation in the 3T3-L1 adipogenesis antagonism assay. RXR antagonism was positively correlated with triglyceride accumulation antagonism and negatively correlated with proliferation antagonism in 3T3-L1 cells. TRβ antagonism was positively correlated with proliferation in hMSCs, while TRβ agonism was negatively associated with triglyceride accumulation antagonism in 3T3-L1 cells. PPARγ antagonism was positively correlated with triglyceride accumulation antagonism in 3T3-L1 cells and negatively with proliferation antagonism. PPARγ agonism, GR antagonism, and GR agonism were not correlated with any adipogenic activities.

The PCA (Fig. 4A) presents the data grouped by the type of chemicals: inorganic, organic or mixture, where mixture is the combination of inorganic and organic chemicals. The antagonist responses of most receptors (RXR, PPARγ, GR and TRβ) were positively correlated to the first dimension, while the agonist responses of all receptors, except GR, were negatively correlated to the first dimension. All the receptors were positively correlated to the second dimension, except GR agonism, which was correlated to the third dimension. Cellular proliferation seemed to be associated with each of the antagonist activities. The hMSC triglyceride accumulation

	RXRa antag	RXRa ag	TRb antag	TRb ag	PPARg antag	PPARg ag	GR antag	GR ag	hMSC TTG	hMSC prolif	hMSC NTG	3T3 TTG	3T3 prolif	3T3 NTG	3T3 TTG antag	3T3 prolif antag	3T3 NTG antag
RXRa antag		-0.32	**0.54**	-0.32	**0.53**	-0.28	**0.51**	0.10	0.26	0.13	0.28	0.45	-0.04	0.30	**0.57**	**-0.70**	0.40
RXRa ag	-0.32		-0.25	**0.73**	**-0.74**	**0.62**	-0.29	**0.57**	-0.33	-0.32	-0.38	0.05	-0.02	-0.15	**-0.47**	0.26	-0.42
TRb antag	**0.54**	-0.25		**-0.48**	0.45	-0.26	0.29	-0.23	0.23	**0.58**	0.17	0.29	-0.14	0.36	0.31	-0.30	0.18
TRb ag	-0.32	**0.73**	**-0.48**		**-0.68**	**0.78**	-0.16	**0.82**	-0.27	-0.30	-0.28	-0.10	-0.22	-0.23	**-0.47**	0.26	-0.36
PPARg antag	**0.53**	**-0.74**	0.45	**-0.68**		**-0.56**	0.18	-0.33	0.25	0.29	0.31	-0.05	0.25	-0.04	**0.56**	**-0.58**	0.39
PPARg ag	-0.28	**0.62**	-0.26	**0.78**	**-0.56**		-0.10	**0.72**	-0.20	-0.01	-0.17	0.01	-0.03	-0.18	-0.24	0.10	-0.22
GR antag	**0.51**	-0.29	0.29	-0.16	0.18	-0.10		-0.19	0.02	0.27	-0.02	0.18	-0.12	0.23	0.39	-0.24	0.41
GR ag	0.10	**0.57**	-0.23	**0.82**	-0.33	**0.72**	-0.19		-0.11	-0.21	-0.11	0.01	-0.16	-0.16	-0.13	-0.20	-0.18
hMSC TTG	0.26	-0.33	0.23	-0.27	0.25	-0.20	0.02	-0.11		0.35	**0.91**	-0.03	-0.32	-0.05	0.35	-0.24	0.37
hMSC prolif	0.13	-0.32	**0.58**	-0.30	0.29	-0.01	0.27	-0.21	0.35		0.26	0.10	-0.21	0.27	0.26	-0.16	0.14
hMSC NTG	0.28	-0.38	0.17	-0.28	0.31	-0.17	-0.02	-0.11	**0.91**	0.26		-0.07	-0.27	-0.13	**0.49**	-0.38	**0.49**
3T3 TTG	0.45	0.05	0.29	-0.10	-0.05	0.01	0.18	0.01	-0.03	0.10	-0.07		0.19	**0.76**	-0.06	0.01	-0.17
3T3 prolif	-0.04	-0.02	-0.14	-0.22	0.25	-0.03	-0.12	-0.16	-0.32	-0.21	-0.27	0.19		-0.24	0.11	-0.12	0.08
3T3 NTG	0.30	-0.15	0.36	-0.23	-0.04	-0.18	0.23	-0.16	-0.05	0.27	-0.13	**0.76**	-0.24		-0.10	0.16	-0.24
3T3 TTG antag	**0.57**	**-0.47**	0.31	**-0.47**	**0.56**	-0.24	0.39	-0.13	0.35	0.26	**0.49**	-0.06	0.11	-0.10		**-0.85**	**0.93**
3T3 prolif antag	**-0.70**	0.26	-0.30	0.26	**-0.58**	0.10	-0.24	-0.20	-0.24	-0.16	-0.38	0.01	-0.12	0.16	**-0.85**		**-0.68**
3T3 NTG antag	0.40	-0.42	0.18	-0.36	0.39	-0.22	0.41	-0.18	0.37	0.14	**0.49**	-0.17	0.08	-0.24	**0.93**	**-0.68**	

Fig. 3. Correlations of receptor bioactivities and adipogenic activities. Spearman's correlations were performed between receptor bioactivities (agonism and antagonism for the retinoid X receptor alpha, thyroid receptor beta, peroxisome proliferator activated receptor gamma, and glucocorticoid receptor) with adipogenic bioactivities (in human mesenchymal stem cells and 3T3-L1 murine pre-adipocytes, assessing both induction of adipogenesis, proliferation, and adipogenesis antagonism, with measurement of rosiglitazone-mediated adipogenesis inhibition). Correlations performed using Prism 9; bolded samples represent significant ($p < 0.05$) correlations, and the color depicts the strength and direction of the correlation. Darker colors represent a stronger correlation, blue coloration depicts positive correlations, and red depicts negative correlations. Abbreviations: ag: agonism; antag: antagonism; hMSC: human mesenchymal stem cell; prolif: proliferation; NTG: normalized triglyceride accumulation; TTG: total triglyceride accumulation. (For interpretation of the references to color in this figure legend, the reader is referred to the web version of this article.)

metrics were associated, but contrary to most of the other variables were negatively correlated with dimension 2. Ellipses demonstrated that data clustered according to the classes of exposure chemicals, with the mixture and organic contaminants overlapping, while the inorganic chemicals clustered separately. The scree plot (Fig. 4B) presents the percentage of explained variance for each dimension. The first two dimensions explained ~57 % of the data variability and the first three explained ~74 %. Dimensions 3–5 together explain ~20 % of the data variability. The correlation matrix (Fig. 4C) was used to examine the percent contribution of each variable to the five dimensions. There is an important contribution of the GR responses to dimensions 3–5, and a lesser contribution of the RXR and TRβ responses to those dimensions.

3.4. Mixture effects of individual contaminants and mixtures

Quantitative determinations of mixture effects were made as has been described in detail previously (Martin et al., 2021). Briefly, predicted effects as per concentration addition were defined for each combination of contaminants; the proportion of expected versus observed effects were used to calculate the toxic effect summation, which was used to define the index of prediction quality (IPQ). IPQ values of > + 100 % were deemed synergistic, values between +100 % and − 100 % were deemed additive, and those < − 100 % were deemed antagonistic. The majority of the mixtures exhibited synergistic effects relative to predicted additive effects for both triglyceride accumulation (Table 1) and for pre-adipocyte proliferation (Table 2) in hMSCs. In every case, concentration addition predicted EC_{10} (concentration that exhibits 10 % of maximal effects) or EC_{50} (concentration that exhibits 50 % of maximal effects) values that were less potent than the observed effects as determined using hMSCs. In most cases, these resulted in IPQ values of > + 100 %, suggesting that most of these mixtures acted synergistically on adipogenic outcomes. The PCB + inorganic mixture and the BFR + inorganic mixture exhibited additive effects when calculated at the EC_{50} level, though these were also synergistic when evaluated at the EC_{10} levels. While effect sizes were considerably lower for pre-adipocyte proliferation, preventing calculation of anything other than EC_{10} values, all of these were synergistic, suggesting significant mixture effects for these various sets of chemicals on both adipogenic outcomes.

3.5. Inorganic contaminant measurements in household dust and correlations with organics and bioactivities

A small set of anonymized dust samples ($n = 30$) was processed for measurement of inorganic contaminants (lead, cadmium, and arsenic). Arsenic was reported in 100 % of the dust samples at concentrations from 0.18 to 41.25 μg/g and a median concentration of 1.52 μg/g (Table 3). Cadmium was reported in 77 % of the dust samples at concentrations from <0.05–1.21 μg/g and a median concentration of 0.20 μg/g. Lead was reported in 100 % of the dust samples at concentrations from 1.06 to 503.49 μg/g and a median of 12.46 μg/g.

4. Discussion

These results demonstrate that complex mixtures of inorganic and organic contaminants, both individually and in various combinations, induce significant disruption of nuclear receptors and promotion of adipogenesis, with the more complex mixtures of contaminants promoting much greater effects than the component contaminants in a number of cases.

Several notable associations were reported between adipogenic and hormone receptor bioactivities. For example, TRβ antagonism was positively correlated with proliferation in hMSCs, supporting its importance as a pro-adipogenic pathway, which we have reported previously (Kassotis et al., 2021a; Kassotis et al., 2019). While limited associations were observed with pro-adipogenic outcomes in 3T3-L1 cells, TRβ/RXR agonism were negatively associated (and RXR antagonism was positively correlated) with triglyceride accumulation antagonism in 3T3-L1 cells, supporting a pro-adipogenic effect of these pathways. We generally reported that across receptor bioactivities and adipogenic activities, mixtures of contaminants promoted greater effects (e.g., more potent and/or more efficacious responses) relative to their individual component contaminants, though only some of these differences were significantly different. Organic

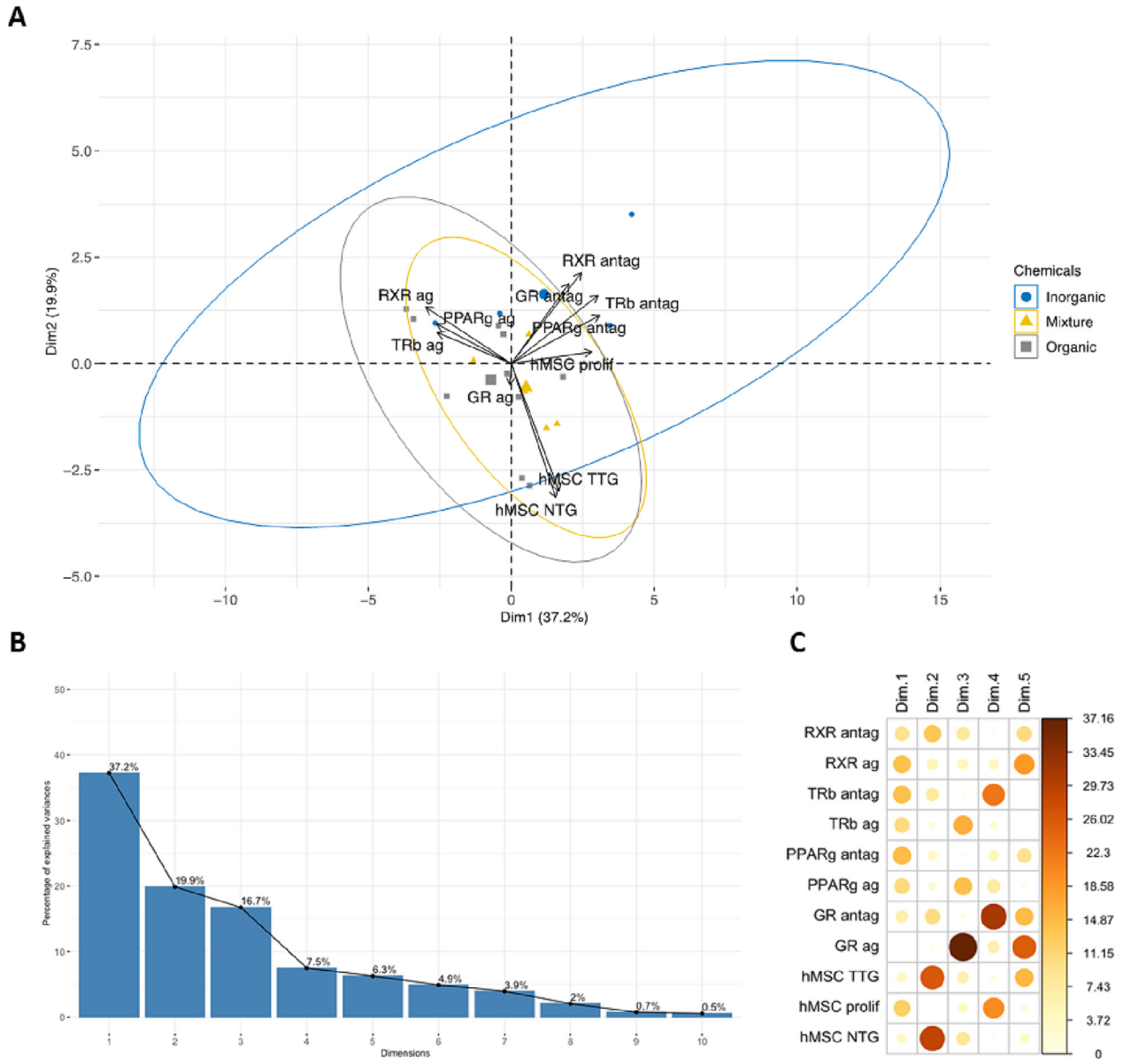

Fig. 4. Associations between receptor bioactivities and adipogenic activities. Principal component analysis (PCA) depicting the relationships between the cellular assays' responses (agonist and antagonist activities for RXRα, PPARγ, GR, and TRβ as well as hMSC triglyceride accumulation and proliferation) and the exposure chemicals/mixtures (inorganic, organic, or mixture). Individual points representing the mean of three biological replicates of each cellular assay ($n = 19$) at the maximal effect concentration are grouped by chemical type, marked by the colored symbols and ellipses (A). The percentage of explained variances for each dimension is presented by the scree plot (B). The contribution in percentage of each variable for the five first dimensions is presented in a correlation plot (C), where darker and larger circles represent a higher contribution of the variable to a dimension, while lighter and smaller circles represent a lower contribution, as presented with the color legend on the right. Abbreviations: GR: Glucocorticoid receptor; PPARγ: peroxisome proliferator activated receptor gamma; RXRα: Retinoid X receptor alpha; TRβ: thyroid hormone receptor beta; ag: agonist; antag: antagonist; hMSC: human mesenchymal stem cell; prolif: proliferation; NTG: normalized triglyceride accumulation; TTG: total triglyceride accumulation.

mixtures tended to exhibit greater effects than individual component chemicals (though not always significantly different), the addition of inorganics often tempered these responses, and the total and environmental mixtures often exhibited bioactivities at a magnitude between the individual contaminants and the mixtures comprised of similar contaminants and inorganics.

The PCA revealed, as expected, a negative association of the agonist and antagonist responses of the receptors analyzed. The PCA also suggested that cellular proliferation of hMSCs might be more associated with the antagonist receptor bioactivities, while triglyceride accumulation was negatively correlated with the receptor bioactivities. It also demonstrates a distribution of the inorganic chemical responses from the organic and the combination mixtures. This suggests that, in exposures to a mixture of organic and inorganic chemicals, the effects caused by the organics were the most potent component in inducing receptor bioactivities. This is particularly interesting given the much lower concentrations of the organics examined here relative to the inorganics in environmental mixtures such as household dust (Table S1) and as examined in the Environmental Mix.

Quantitative determinations of mixture effects suggested that the hMSC adipogenic effects (both triglyceride accumulation and pre-adipocyte proliferation) were synergistic as compared to the predicted effects defined by concentration addition. While several of the mixtures at the EC_{50} effect level (PFAS + inorganics and BFRs + inorganics) exhibited lower-level (deemed additive) effects, their effects at the EC_{10} level were strongly synergistic, suggesting that overall, these collections of adipogenic contaminants acted in a synergistic manner. In support of synergistic effects, we

Table 1
Mixture effect calculations for triglyceride accumulation in human mesenchymal stem cells.

Activity level	Effective concentration $EC_{x_{mix}}$ (M)			
Level *x*	Observed	Predicted by CA	Index of Prediction Quality (IPQ)	Determination
PFAS mix: two PFAS				
10 %	0.0025	0.15135	5954 %	Synergistic
50 %	0.2	0.53992	170 %	Synergistic
BFR mix: two BFRs				
10 %	0.0008	2.45902	307,277 %	Synergistic
50 %	7.5	10,909.1	145,355 %	Synergistic
PCB mix: two PCBs				
10 %	0.00075	0.00383	411 %	Synergistic
50 %	0.015	8.97756	59,750 %	Synergistic
PFAS + Inorganic mix: two PFAS and three inorganics				
10 %	0.018	0.04183	132 %	Synergistic
50 %	1.2	2.38778	99 %	Additive
BFR + Inorganic mix: two BFRs and three inorganics				
10 %	0.0025	0.04667	1767 %	Synergistic
50 %	2	2.43123	22 %	Additive
PCB + Inorganic mix: two PCBs and three inorganics				
10 %	0.003	0.00795	165 %	Synergistic
50 %	0.185	2.19378	1086 %	Synergistic
Inorganic mix: three inorganics				
10 %	0.00035	0.02850	8044 %	Synergistic
50 %	0.1	1.47360	1374 %	Synergistic
Organic mix: six organics comprised of 2 PFAS, 2 BFRs, and 2 PCBs				
10 %	0.0018	0.01117	520 %	Synergistic
50 %	0.9	22.9805	2453 %	Synergistic
Total mix: all six organics and three inorganics				
10 %	0.0033	0.01415	329 %	Synergistic
50 %	0.5	3.92364	685 %	Synergistic
Enviro mix: all six organics and three inorganics				
10 %	0.0015	0.02713	1709 %	Synergistic
50 %	0.3	1.47174	391 %	Synergistic

Mixture effect calculations performed to describe deviations from observed effects. All mixtures were equimolar concentrations of constituent chemicals except for the environmental mixture, which had the inorganic constituent chemicals at 100 × the concentrations of the organic contaminants, with both sets individually at equimolar concentrations. Observed effects are the concentration in micromolar at which the 10 % or 50 % effect levels were observed for each mixture. Concentration addition predictions were calculated as described in methods and according to standard protocols and are provided as micromolar concentrations at which mixtures are predicted to have 10 % or 50 % effect levels. Index of predictive quality is a method to create a linearized symmetric scale to determine deviations of observed results from predicted, and are used to define whether the effects are "synergistic" (greater than predicted), "additive" (approximately as per predicted values via concentration addition), or "antagonistic" (less than predicted).

saw independent determinations of synergy for two separate measures of pro-adipogenic activity in the human MSC model (both triglyceride accumulation and pre-adipocyte proliferation), which supports that these contaminants elicited effects that occurred at significantly more potent concentrations than would be anticipated by the concentration addition effect model. Importantly, some (but not all) of these mixture effects were significantly greater than the effects of each of their components.

Several limitations are inherent in our mixture approach; our dose response curves utilized 4–5 tested concentrations at 10-fold concentration gaps, which hinders our ability to define an appropriate curve fit and limits our subsequent ability to define a robust predicted mixture effect concentration, particularly for the 50 % effect level. Future research should evaluate effects using independent action or other more descriptive statistical models that may be better suited to these complex mixtures. An inherent limitation of both concentration addition and independent action is that there is no capacity to account for opposing effects. For example, chemicals that individually act to inhibit adipogenesis would not be properly accounted for in these mixture models, whereas weighted quantile sum or quantile g computation models are able to define both positive and negative effects on mixture outcomes such as this – though also generally require much greater sample sizes than are possible in a toxicological dataset such as described here. Further testing is warranted to define how these chemicals may interact to promote greater than anticipated endocrine and/or metabolic health outcomes.

Concerning discordance was observed between the effects in 3T3-L1 pre-adipocytes and hMSCs. Neither triglyceride accumulation nor proliferation in the hMSC model were positively associated with these pro-adipogenic metrics in 3T3-L1 cells. Interestingly, antagonistic responses in this assay were positively correlated with triglyceride accumulation in hMSCs, reflecting a distinct metabolic disrupting profile between these models. We recently reported strong concordance between 3T3-L1 and hMSCs for a set of alkylphenol polyethoxylates (Kassotis et al., 2022a), suggesting that this concordance/discordance may be specific to certain pathways and/or sets of contaminants. We also recently reported that there is poor reproducibility between laboratories for 3T3-L1 cells, in part due to cell line source and in part due to differences in differentiation protocols used between laboratories (Kassotis et al., 2021b). Differences in species (human versus murine), sex, stage of cell line commitment (multipotent progenitors versus committed pre-adipocytes), and differentiation induction protocols (i.e., both component chemicals in differentiation media as well as the differentiation time-course) may all contribute to the differences in adipogenic responses observed here. Importantly, there is an incomplete understanding of how these in vitro responses translate into functional in vivo health outcomes (Kassotis et al., 2022b), which should be explored further in future animal research.

We also reported select inorganic contaminant concentrations for a subset of dust samples collected from households in central NC. Specifically, levels of arsenic, cadmium, and lead had median concentrations of approximately 1.5, 0.20, and 12.5 μg/g, with detection frequencies of 100 %, 77 %, and 100 %, respectively. These concentrations of arsenic are in the same range as other median concentrations reported previously (1.6–62 μg/g; Table S1). Median cadmium concentrations of 0.2 were 10-fold or more lower than those reported previously (1.6–1900 μg/g; Table S1). Median lead concentrations of 12.5 μg/g were generally lower than those reported previously (49–573 μg/g; Table S1). While this was a small subset of dust samples, the concentrations generally agreed with those measured elsewhere with the possible exception of cadmium (literature median values of 1.6–4.3 μg/g). More widespread testing would need to be performed to confirm whether concentrations are significantly different than those reported in other studies.

Several previous publications by our group have reported on adipogenic activity from complex mixtures of contaminants isolated from household dust samples (Kassotis et al., 2021a; Kassotis et al., 2019). These publications have consistently reported adipogenic activity in ~90 % of samples across a broad range of concentrations, even at concentrations <10 μg dust equivalence per well. While we have consistently reported significant associations with specific organic contaminants, we have not been able to account for the total magnitude of the adipogenic and/or receptor bioactivities. These samples are extremely complex, with preliminary research demonstrating the presence of thousands of different contaminants in household dust (Ferguson et al., 2015; Hilton et al., 2010). We previously utilized a cutting-edge mixtures approach using quantile g-computation (Kassotis et al., 2021a), which found that contaminant mixtures were strongly and positively associated with triglyceride accumulation, yet did not account for the total magnitude of the adipogenic activity exhibited by the extracts. We also observed no significant mixture effects for pre-adipocyte proliferation or for thyroid receptor antagonism, suggesting that other contaminants may be responsible for some of the missing complexity of this activity. Herein we describe a previously unexplored contribution, the co-occurring inorganic contaminants present in household dust

Table 2
Mixture effect calculations for pre-adipocyte proliferation in human mesenchymal stem cells.

Activity level	Effective concentration ECx_{mix} (M)			
Level x	Observed	Predicted by CA	Index of Prediction Quality (IPQ)	Determination
PFAS mix: two PFAS at equimolar concentrations				
10 %	0.001	0.03111	3011 %	Synergistic
BFR mix: two BFRs at equimolar concentrations				
10 %	0.00027	2.45902	910,647 %	Synergistic
PCB mix: two PCBs at equimolar concentrations				
10 %	0.000025	0.00383	15,219 %	Synergistic
PFAS + Inorganic mix: two PFAS and three inorganics at equimolar concentrations				
10 %	0.011	0.04183	280 %	Synergistic
BFR + Inorganic mix: two BFRs and three inorganics at equimolar concentrations				
10 %	0.0012	0.04667	3789 %	Synergistic
PCB + Inorganic mix: two PCBs and three inorganics at equimolar concentrations				
10 %	0.0025	0.00795	218 %	Synergistic
Inorganic mix: three inorganics at equimolar concentrations				
10 %	0.0055	0.02850	418 %	Synergistic
Organic mix: six organics comprised of 2 PFAS, 2 BFRs, and 2 PCBs at equimolar concentrations				
10 %	0.0027	0.01117	314 %	Synergistic
Total mix: all six organics and three inorganics at equimolar concentrations				
10 %	0.0013	0.01415	988 %	Synergistic
Enviro mix: all six organics and three inorganics at environmental ratios as described above				
10 %	0.00045	0.02713	5930 %	Synergistic

Mixture effect calculations performed to describe deviations from observed effects. All mixtures were equimolar concentrations of constituent chemicals except for the environmental mixture, which had the inorganic constituent chemicals at 100× the concentrations of the organic contaminants, with both sets individually at equimolar concentrations. Observed effects are the concentration in micromolar at which the 10 % or 50 % effect levels were observed for each mixture. Concentration addition predictions were calculated as described in methods and according to standard protocols and are provided as micromolar concentrations at which mixtures are predicted to have 10 % or 50 % effect levels. Index of predictive quality is a method to create a linearized symmetric scale to determine deviations of observed results from predicted, and are used to define whether the effects are "synergistic" (greater than predicted), "additive" (approximately as per predicted values via concentration addition), or "antagonistic" (less than predicted).

Table 3
Inorganic contaminant concentrations in dust extracts.

Sample ID	Arsenic (μg/g)	Cadmium (μg/g)	Lead (μg/g)
2	0.53	0.09	7.74
3	0.33	<0.05	1.06
13	0.23	0.13	11.16
33	0.18	<0.05	2.32
46	5.20	0.30	14.35
48	1.38	0.09	20.93
49	0.86	0.04	7.07
73	0.54	0.19	13.76
75	41.25	0.28	98.27
76	1.22	1.21	503.49
77	1.47	0.25	8.07
79	1.93	<0.05	14.14
80	12.85	0.51	3.58
81	0.48	0.09	15.63
83	39.54	0.20	24.63
85	1.70	0.17	15.45
94	1.12	<0.05	1.39
97	2.22	0.16	10.70
102	1.57	<0.05	9.61
110	2.31	0.10	10.77
115	3.26	<0.05	6.05
120	2.21	0.49	10.44
121	1.46	0.22	67.99
122	3.48	0.35	47.08
123	5.61	0.17	39.99
132	1.18	0.26	47.63
134	1.20	0.07	17.29
138	7.96	0.34	18.02
139	0.98	0.50	8.58
149	1.95	<0.05	7.22
Mean	4.87	0.27	35.48
Median	1.52	0.20	12.46
Detection Frequency	100.0 %	76.7 %	100.0 %
MDL (ppb)	0.05	0.05	0.05

Analytical results and descriptive statistics for targeted inorganic contaminant concentrations for n = 30 residential household dust samples collected from central NC. Detection frequency across these dust extracts is provided for all chemicals, the mean and median concentrations, and the MDL (method detection limit). <LOQ = concentrations below the MDL for a specific dust extract.

extracts, albeit examining only a limited subset of inorganic contaminants that may be present in this matrix. Further research is needed with larger sample sizes to explore potential mixture effects of organic and inorganic contaminant mixtures in environmental matrices.

Appreciably, there are some inherent limitations in our approach. We evaluated receptor bioactivities for the contaminants and their mixtures using cell lines that express the specific receptors endogenously. While these are more likely to exhibit effects in a physiologically relevant manner, there may also be tissue-specific effects that limit our ability to generalize these results to what may be observed using a pre-adipocyte or MSC model. While our equimolar assessment of the contaminants (and our skewed Enviro Mix, designed to approximate the 100-fold variations between inorganic and organic concentrations) was designed for ease of mixture calculations and straightforward progression of effects, future efforts should focus on realistic mixtures reflecting actual median concentrations of each of the individual contaminants in household dust samples (Table S1). More comprehensive coverage of concentrations would also support curve fitting, and potentially more accurate determinations of potencies (e.g., EC_{10}, EC_{50} values), which isn't feasible for complex mixtures of this type for multiple endpoints. This can be viewed as an exploratory mixture assessment, which can and should be followed up on with more comprehensive testing on certain specific interactions, allowing for a more detailed assessment of the causal mechanisms and a more fine-tuned approach to mixture effects across a more comprehensive tested concentration range. Similarly, we have also focused here on four adipogenic pathways that are very commonly involved in pro- and/or anti-adipogenic responses. While there were not clear associations present in the correlation analysis for triglyceride accumulation, the majority of the chemicals and mixtures active in hMSC cells also had activity at overlapping concentrations on pro-adipogenic receptor pathways. It is also important to recognize, as we have detailed previously (Heindel et al., 2022; Kassotis et al., 2022b; Lustig et al., 2022), that there are numerous pro-adipogenic mechanisms; examining all of these would be beyond the scope of any one study. It is also likely that co-disruption of multiple adipogenic activities at low levels can also result in markedly increased effects when considered in combination, a common phenomenon for mixture assessments (Rajapakse et al., 2002; Silva et al., 2002; Thrupp et al., 2018).

In summary, we report putatively synergistic and significantly increased effects on adipogenic outcomes for several mixtures of organic and inorganic contaminants. These apparent greater than anticipated effects across diverse chemical classes suggests that these combinations could potentially account for the robust adipogenic activity exhibited by small concentrations of residential household dust reported previously (Kassotis et al., 2021a; Kassotis et al., 2017a; Kassotis et al., 2019). Future research should perform more detailed evaluations of specific endpoints and chemical sets, evaluate whether these effects persist into whole organisms, whether they are better predicted using other mixture models, and whether different inorganics may temper or otherwise modulate the bioactivities of diverse organic contaminants and their mixtures. Future research should also substantiate previous house dust findings using this and other hMSC or pre-adipocyte models, which will support the findings here and may lend increased relevance to human health outcomes.

Funding

Project supported by awards (R00 ES030405 and P30 ES020957) from the National Institute of Environmental Health Sciences (NIEHS).

Author contributions

CDK conceptualized study and planned for study implementation. CDK and YTC performed all bioassays; JAB and JW performed all analytical processing and analysis; RB performed statistical analysis; SH, RB, MKL, KH assisted with writing and all authors provided critical feedback and edits.

Data availability

Data will be made available on request.

Declaration of competing interest

The authors declare the following financial interests/personal relationships which may be considered as potential competing interests: Christopher Kassotis reports financial support was provided by National Institute of Environmental Health.

Appendix A. Supplementary data

Supplementary data to this article can be found online at https://doi.org/10.1016/j.scitotenv.2023.162587.

References

Chang, C.J., Terrell, M.L., Marcus, M., Marder, M.E., Panuwet, P., Ryan, P.B., et al., 2020. Serum concentrations of polybrominated biphenyls (PBBs), polychlorinated biphenyls (PCBs) and polybrominated diphenyl ethers (PBDEs) in the Michigan PBB registry 40 years after the PBB contamination incident. Environ. Int. 137, 105526.

Chou, P.-H., Lee, C.-H., Ko, F.-C., Lin, Y.-J., Kawanishi, M., Yagi, T., et al., 2015. Detection of hormone-like and genotoxic activities in indoor dust from Taiwan using a battery of in vitro bioassays. Aerosol Air Qual. Res. 15, 1412–1421.

Dallaire, F., Dewailly, E., Muckle, G., Ayotte, P., 2003. Time trends of persistent organic pollutants and heavy metals in umbilical cord blood of inuit infants born in nunavik (Quebec, Canada) between 1994 and 2001. Environ. Health Perspect. 111, 1660–1664.

Di Carlo, F.J., Seifter, J., DeCarlo, V.J., 1978. Assessment of the hazards of polybrominated biphenyls. Environ. Health Perspect. 23, 351–365.

Diamanti-Kandarakis, E., Bourguignon, J.P., Giudice, L.C., Hauser, R., Prins, G.S., Soto, A.M., et al., 2009. Endocrine-disrupting chemicals: an Endocrine Society scientific statement. Endocr. Rev. 30, 293–342.

Dixon, S.L., Gaitens, J.M., Jacobs, D.E., Strauss, W., Nagaraja, J., Pivetz, T., et al., 2009. Exposure of U.S. Children to residential dust lead, 1999–2004: II. The contribution of lead-contaminated dust to children's blood lead levels. Environ. Health Perspect. 117, 468–474.

Environmental Protection Agency (EPA), 2017. Exposure Factors Handbook Chapter 5 (Update): Soil and Dust Ingestion. In: EPA, U.S. (Ed.), 2017 Update, Washington, DC, 2011 Edition (Final).

Ermler, S., Scholze, M., Kortenkamp, A., 2011. The suitability of concentration addition for predicting the effects of multi-component mixtures of up to 17 anti-androgens with varied structural features in an in vitro AR antagonist assay. Toxicol. Appl. Pharmacol. 257, 189–197.

Fang, M., Webster, T.F., Ferguson, P.L., Stapleton, H.M., 2015a. Characterizing the peroxisome proliferator-activated receptor (PPARgamma) ligand binding potential of several major flame retardants, their metabolites, and chemical mixtures in house dust. Environ. Health Perspect. 123, 166–172.

Fang, M., Webster, T.F., Stapleton, H.M., 2015b. Activation of human peroxisome proliferator-activated nuclear receptors (PPARgamma1) by semi-volatile compounds (SVOCs) and chemical mixtures in indoor dust. Environ. Sci. Technol. 49, 10057–10064.

Fang, M., Webster, T.F., Stapleton, H.M., 2015c. Effect-directed analysis of human peroxisome proliferator-activated nuclear receptors (PPARgamma1) ligands in indoor dust. Environ. Sci. Technol. 49, 10065–10073.

Ferguson, P.L., Vogler, B., Stapleton, H.M., 2015. Non-targeted analysis to assess human exposure to semi-volatile organic contaminants in the indoor environment. Proceedings of the 63rd ASMS Conference on Mass Spectrometry and Allied Topics, St. Louis, MO.

Fox, J., Weisberg, S., 2019. An R Companion to Applied Regression. Sage, Third Edition, Thousand Oaks, CA.

Fraser, A.J., Webster, T.F., Watkins, D.J., Nelson, J.W., Stapleton, H.M., Calafat, A.M., et al., 2012. Polyfluorinated compounds in serum linked to indoor air in office environments. Environ. Sci. Technol. 46, 1209–1215.

Gore, A.C., Chappell, V.A., Fenton, S.E., Flaws, J.A., Nadal, A., Prins, G.S., et al., 2015. EDC-2: the Endocrine Society's second scientific statement on endocrine-disrupting chemicals. Endocr. Rev. 36, E1–E150.

Green, A.J., Hoyo, C., Mattingly, C.J., Luo, Y., Tzeng, J.Y., Murphy, S.K., et al., 2018. Cadmium exposure increases the risk of juvenile obesity: a human and zebrafish comparative study. Int. J. Obes. 42, 1285–1295.

Heindel, J.J., vom Saal, F.S., Blumberg, B., Bovolin, P., Calamandrei, G., Ceresini, G., et al., 2015. Parma consensus statement on metabolic disruptors. Environ. Health 14, 54.

Heindel, J.J., Blumberg, B., Cave, M., Machtinger, R., Mantovani, A., Mendez, M.A., et al., 2017. Metabolism disrupting chemicals and metabolic disorders. Reprod. Toxicol. 68, 3–33.

Heindel, J.J., Howard, S., Agay-Shay, K., Arrebola, J.P., Audouze, K., Babin, P.J., et al., 2022. Obesity II: establishing causal links between chemical exposures and obesity. Biochem. Pharmacol. 199, 115015.

Hilton, D.C., Jones, R.S., Sjodin, A., 2010. A method for rapid, non-targeted screening for environmental contaminants in household dust. J. Chromatogr. A 1217, 6851–6856.

Hoffman, K., Lorenzo, A., Butt, C.M., Hammel, S.C., Henderson, B.B., Roman, S.A., et al., 2017. Exposure to flame retardant chemicals and the occurrence and severity of papillary thyroid cancer. Environ. Int. 107, 235–242.

Hoffman, K., Hammel, S.C., Phillips, A.L., Lorenzo, A.M., Chen, A., Calafat, A.M., et al., 2018. Biomarkers of exposure to SVOCs in children and their demographic associations: the TESIE study. Environ. Int. 119, 26–36.

Houlihan, J., Kropp, T., Wiles, R., Gray, S., Campbell, C., 2005. BodyBurden: The Pollution in Newborns. Environmental Working Group.

Jones, D.H., Platonow, N.S., Safe, S., 1975. Contamination of agricultural products by halogenated biphenyls. Can. Vet. J. 16, 349–356.

Kademoglou, K., Xu, F., Padilla-Sanchez, J.A., Haug, L.S., Covaci, A., Collins, C.D., 2017. Legacy and alternative flame retardants in norwegian and UK indoor environment: implications of human exposure via dust ingestion. Environ. Int. 102, 48–56.

Kassambara, A., Mundt, F., 2020. factoextra: Extract and Visualize the Results of Multivariate Data Analyses. R package version 1.0.7. Available from https://CRAN.R-project.org/package=factoextra.

Kassotis, C.D., Tillitt, D.E., Lin, C.H., McElroy, J.A., Nagel, S.C., 2016. Endocrine-disrupting chemicals and oil and Natural gas operations: potential environmental contamination and recommendations to assess complex environmental mixtures. Environ. Health Perspect. 124, 256–264.

Kassotis, C.D., Hoffman, K., Stapleton, H.M., 2017:. Characterization of adipogenic activity of semi-volatile indoor contaminants and house dust. Environ Sci Technol 51, 8735–8745.

Kassotis, C.D., Masse, L., Kim, S., Schlezinger, J.J., Webster, T.F., Stapleton, H.M., 2017b. Characterization of adipogenic Chemicals in Three Different Cell Culture Systems: implications for reproducibility based on cell source and handling. Sci. Rep. 7, 42104.

Kassotis, C.D., Kollitz, E.M., Ferguson, P.L., Stapleton, H.M., 2018a. Nonionic ethoxylated surfactants induce adipogenesis in 3T3-L1 cells. Toxicol. Sci. 162, 124–136.

Kassotis, C.D., Nagel, S.C., Stapleton, H.M., 2018b. Unconventional oil and gas chemicals and wastewater-impacted water samples promote adipogenesis via PPARγ-dependent and independent mechanisms in 3T3-L1 cells. Sci. Total Environ. 640-641, 1601–1610.

Kassotis, C.D., Kollitz, E.M., Hoffman, K., Sosa, J.A., Stapleton, H.M., 2019. Thyroid receptor antagonism as a contributory mechanism for adipogenesis induced by environmental mixtures in 3T3-L1 cells. Sci. Total Environ. 666, 431–444.

Kassotis, C.D., Herkert, N.J., Hammel, S.C., Hoffman, K., Xia, Q., Kullman, S.W., et al., 2020. Thyroid receptor antagonism of chemicals extracted from personal silicone wristbands within a papillary thyroid cancer pilot study. Environ. Sci. Technol. 54, 15296–15312.

Kassotis, C.D., Hoffman, K., Phillips, A.L., Zhang, S., Cooper, E.M., Webster, T.F., et al., 2021a. Characterization of adipogenic, PPARgamma, and TRbeta activities in house dust extracts and their associations with organic contaminants. Sci. Total Environ. 758, 143707.

Kassotis, C.D., Hoffman, K., Volker, J., Pu, Y., Veiga-Lopez, A., Kim, S.M., et al., 2021b. Reproducibility of adipogenic responses to metabolism disrupting chemicals in the 3T3-L1 pre-adipocyte model system: an interlaboratory study. Toxicology 461, 152900.

Kassotis, C.D., Vom Saal, F.S., Babin, P.J., Lagadic-Gossmann, D., Le Mentec, H., Blumberg, B., et al., 2022b. Obesity III: obesogen assays: limitations, strengths, and new directions. Biochem. Pharmacol. 199, 115014.

Kassotis, C.D., LeFauve, M.K., Chiang, Y.T., Knuth, M.M., Schkoda, S., Kullman, S.W., 2022;;. Nonylphenol polyethoxylates enhance adipose deposition in developmentally exposed zebrafish. Toxics 10.

Kollitz, E.M., Kassotis, C.D., Hoffman, K., Ferguson, P.L., Sosa, J.A., Stapleton, H.M., 2018. Chemical mixtures isolated from house dust disrupt thyroid receptor β (TRβ) signaling. Environ. Sci. Technol. 52, 11857–11864.

Landrigan, P.J., Sonawane, B., Mattison, D., McCally, M., Garg, A., 2002. Chemical contaminants in breast milk and their impacts on children's health: an overview. Environ. Health Perspect. 110, A313–A315.

Li, X., Ycaza, J., Blumberg, B., 2011. The environmental obesogen tributyltin chloride acts via peroxisome proliferator activated receptor gamma to induce adipogenesis in murine 3T3-L1 preadipocytes. J. Steroid Biochem. Mol. Biol. 127, 9–15.

Lustig, R.H., Collier, D., Kassotis, C., Roepke, T.A., Kim, M.J., Blanc, E., et al., 2022. Obesity I: overview and molecular and biochemical mechanisms. Biochem. Pharmacol. 199, 115012.

Lyche, J.L., Nourizadeh-Lillabadi, R., Almaas, C., Stavik, B., Berg, V., Skare, J.U., et al., 2010. Natural mixtures of persistent organic pollutants (POP) increase weight gain, advance puberty, and induce changes in gene expression associated with steroid hormones and obesity in female zebrafish. J. Toxicol. Environ. Health A 73, 1032–1057.

Martin, O., Scholze, M., Ermler, S., McPhie, J., Bopp, S., Kienzler, A., et al., 2021. Ten years of research on synergisms and antagonisms in chemical mixtures: a systematic review and quantitative reappraisal of mixture studies. Environ. Int. 146.

Martini, C.N., Gabrielli, M., Bonifacino, G., Codesido, M.M., Vila, M.D.C., 2018. Lead enhancement of 3T3-L1 fibroblasts differentiation to adipocytes involves ERK, C/EBPbeta and PPARgamma activation. Mol. Cell. Biochem. 437, 37–44.

Mitro, S.D., Dodson, R.E., Singla, V., Adamkiewicz, G., Elmi, A.F., Tilly, M.K., et al., 2016. Consumer product chemicals in indoor dust: a quantitative meta-analysis of U.S. studies. Environ Sci Technol 50, 10661–10672.

Mogensen, U.B., Grandjean, P., Nielsen, F., Weihe, P., Budtz-Jorgensen, E., 2015. Breastfeeding as an exposure pathway for perfluorinated alkylates. Environ. Sci. Technol 49, 10466–10473.

Phillips, A.L., Hammel, S.C., Hoffman, K., Lorenzo, A.M., Chen, A., Webster, T.F., et al., 2018. Children's residential exposure to organophosphate ester flame retardants and plasticizers: investigating exposure pathways in the TESIE study. Environ. Int. 116, 176–185.

Rajapakse, N., Silva, E., Kortenkamp, A., 2002. Combining xenoestrogens at levels below individual no-observed-effect concentrations dramatically enhances steroid hormone action. Environ. Health Perspect. 110, 917–921.

Rajapakse, N., Silva, E., Scholze, M., Kortenkamp, A., 2004. Deviation from additivity with estrogenic mixtures containing 4-nonylphenol and 4-tert-octylphenol detected in the E-SCREEN assay. Environ. Sci. Technol. 38, 6343–6352.

Rasmussen, P.E., Levesque, C., Chenier, M., Gardner, H.D., Jones-Otazo, H., Petrovic, S., 2013. Canadian house dust study: population-based concentrations, loads and loading rates of arsenic, cadmium, chromium, copper, nickel, lead, and zinc inside urban homes. Sci. Total Environ. 443, 520–529.

Robertson, L.W., Chynoweth, D.P., 1975. Another halogenated hydrocarbon. Environ. Sci. Policy Sustain. Dev. 17, 25–27.

Rodriguez, K.F., Mellouk, N., Ungewitter, E.K., Nicol, B., Liu, C., Brown, P.R., et al., 2020. In utero exposure to arsenite contributes to metabolic and reproductive dysfunction in male offspring of CD-1 mice. Reprod. Toxicol. 95, 95–103.

Rudel, R.A., Camann, D.E., Spengler, J.D., Korn, L.R., Brody, J.G., 2003. Phthalates, alkylphenols, pesticides, polybrominated diphenyl ethers, and other endocrine-disrupting compounds in indoor air and dust. Environ. Sci. Technol. 37, 4543–4553.

Schilmann, A., Lacasana, M., Blanco-Munoz, J., Aguilar-Garduno, C., Salinas-Rodriguez, A., Flores-Aldana, M., et al., 2010. Identifying pesticide use patterns among flower growers to assess occupational exposure to mixtures. Occup. Environ. Med. 67, 323–329.

Shao, X., Wang, M., Wei, X., Deng, S., Fu, N., Peng, Q., et al., 2016. Peroxisome proliferator-activated receptor-gamma: master regulator of adipogenesis and obesity. Curr. Stem Cell Res. Ther. 11, 282–289.

Silva, E., Rajapakse, N., Kortenkamp, A., 2002. Something from "nothing"–eight weak estrogenic chemicals combined at concentrations below NOECs produce significant mixture effects. Environ. Sci. Technol. 36, 1751–1756.

Stapleton, H.M., Dodder, N.G., Offenberg, J.H., Schantz, M.M., Wise, S.A., 2005. Polybrominated diphenyl ethers in house dust and clothes dryer lint. Environ. Sci. Technol. 39, 925–931.

Stapleton, H.M., Harner, T., Shoeib, M., Keller, J.M., Schantz, M.M., Leigh, S.D., et al., 2006. Determination of polybrominated diphenyl ethers in indoor dust standard reference materials. Anal. Bioanal. Chem. 384, 791–800.

Stapleton, H.M., Allen, J.G., Kelly, S.M., Konstantinov, A., Klosterhaus, S., Watkins, D., et al., 2008. Alternate and new brominated flame retardants detected in U.S. house dust. Environ. Sci. Technol. 42, 6910–6916.

Stapleton, H.M., Klosterhaus, S., Eagle, S., Fuh, J., Meeker, J.D., Blum, A., et al., 2009. Detection of organophosphate flame retardants in furniture foam and U.S. House dust. Environ Sci Technol 43, 7490–7495.

Stapleton, H.M., Eagle, S., Sjodin, A., Webster, T.F., 2012. Serum PBDEs in a North Carolina toddler cohort: associations with handwipes, house dust, and socioeconomic variables. Environ. Health Perspect. 120, 1049–1054.

Suzuki, G., Takigami, H., Nose, K., Takahashi, S., Asari, M., Sakai, S., 2007. Dioxin-like and transthyretin-binding compounds in indoor dusts collected from Japan: average daily dose and possible implications for children. Environ Sci Technol 41, 1487–1493.

Suzuki, G., Tue, N.M., Malarvannan, G., Sudaryanto, A., Takahashi, S., Tanabe, S., et al., 2013. Similarities in the endocrine-disrupting potencies of indoor dust and flame retardants by using human osteosarcoma (U2OS) cell-based reporter gene assays. Environ Sci Technol 47, 2898–2908.

Taxvig, C., Dreisig, K., Boberg, J., Nellemann, C., Schelde, A.B., Pedersen, D., et al., 2012. Differential effects of environmental chemicals and food contaminants on adipogenesis, biomarker release and PPARgamma activation. Mol. Cell. Endocrinol. 361, 106–115.

Thrupp, T.J., Runnalls, T.J., Scholze, M., Kugathas, S., Kortenkamp, A., Sumpter, J.P., 2018. The consequences of exposure to mixtures of chemicals: something from 'nothing' and 'a lot from a little' when fish are exposed to steroid hormones. Sci. Total Environ. 619–620, 1482–1492.

Tung, E.W., Boudreau, A., Wade, M.G., Atlas, E., 2014. Induction of adipocyte differentiation by polybrominated diphenyl ethers (PBDEs) in 3T3-L1 cells. PLoS One 9, e94583.

Watkins, D.J., McClean, M.D., Fraser, A.J., Weinberg, J., Stapleton, H.M., Sjodin, A., et al., 2011. Exposure to PBDEs in the office environment: evaluating the relationships between dust, handwipes, and serum. Environ. Health Perspect. 119, 1247–1252.

Watkins, D.J., McClean, M.D., Fraser, A.J., Weinberg, J., Stapleton, H.M., Sjodin, A., et al., 2012. Impact of dust from multiple microenvironments and diet on PentaBDE body burden. Environ Sci Technol 46, 1192–1200.

Watkins, D.J., McClean, M.D., Fraser, A.J., Weinberg, J., Stapleton, H.M., Webster, T.F., 2013. Associations between PBDEs in office air, dust, and surface wipes. Environ. Int. 59, 124–132.

Watkins, A.M., Wood, C.R., Lin, M.T., Abbott, B.D., 2015. The effects of perfluorinated chemicals on adipocyte differentiation in vitro. Mol. Cell. Endocrinol. 400, 90–101.

Wei, T., Simko, V., 2021. R package 'corrplot': visualization of a correlation matrix (version 0.92). Available from https://github.com/taiyun/corrplot.

Wickham, H., 2016. ggplot2: Elegant Graphics for Data Analysis. Springer-Verlag, New York.